ADVANCED FUNCTIONAL MATERIALS
www.afm-journal.de

Influence of Pendant Group on Mobility of Organic Thin Film Transistor in Correlation with Reorganization Energy of Molecules

Kalyani Patrikar, Nakul Jain, Dwaipayan Chakraborty, Priya Johari, Valipe Ramgopal Rao, and Dinesh Kabra**

Charge transport properties of common donor copolymers in organic photovoltaics, poly({4,8-bis[(2-ethylhexyl)oxy]benzo[1,2-b:4,5-b′] dithiophene-2,6-diyl}{3-fluoro-2-[(2-ethylhexyl)carbonyl]thieno[3,4-b] thiophenediyl}) (PTB7) and poly([2,6′-4,8-di(5-ethylhexylthienyl)benzo[1,2-b;3,3-b]dithiophene]{3-fluoro-2[(2-ethylhexyl) carbonyl]thieno[3,4-b] thiophenediyl}) (PTB7-Th), with molecular structures differing only in the pendant group, are studied. This is the first report of field-effect transistor mobility (μ_{FET}) of PTB7-Th (0.14 $cm^2 V^{-1} s^{-1}$) and the highest μ_{FET} for PTB7 (0.01 $cm^2 V^{-1} s^{-1}$). μ_{FET} of PTB7-Th is found to be almost one order of magnitude higher than PTB7. To understand the influence of molecular structure on charge transport, hole reorganization energy (λ_h) is calculated from first-principles. λ_h of PTB7-Th (≈150 meV) is found to be lower than PTB7 (≈346 meV). Further, the ratio of hopping rate versus square of charge transfer integral calculated from Marcus theory using λ_h for these systems is found to indicate a higher rate of hole transfer across dimers or homojunction interface for PTB7-Th. These results are supplemented by experimentally determined λ using bulk-heterojunction organic solar cells, where $\lambda_{PTB7\text{-}Th}$≈200 meV and λ_{PTB7}≈310 meV follow a similar trend. The effective hole-mobility estimation from BHJ devices correlates well with these λ values. This study provides understanding of charge transport properties via reorganization energy, as a function of pendant group without altering the backbone of the chains.

1. Introduction

Conjugated polymers have found applications in various electronic and optoelectronic devices, such as organic field-effect transistors (OFETs), polymer light-emitting diodes (PLEDs), and organic photovoltaics (OPVs).[1,2] Among these devices, OPVs and OFETs are still a big part of academic research community, as expected parameters in terms of efficiency for solar cells and mobility for OFETs are yet to reach the adequate level for practical use. In recent times, the solar cell efficiency of polymer solar cells has exceeded the value of 14% in single junction geometry.[3] This has happened due to advances in molecular design to create polymers which not only had right interfacial properties with acceptor fullerene molecules, but also efficient charge transport properties for holes.[4,5] Values of field effect mobility for polymer semiconductors have also increased due to efforts in molecular design and processing conditions. A recent such development has been synthesis of donor–acceptor (DA) copolymers, repeat units of which comprise electron-rich donor and electron-deficient acceptor sub-units. DA polymers have achieved mobility exceeding 1 $cm^2 V^{-1} s^{-1}$, due to modulation of band gap according to composition of donor and acceptor units.[6]

Charge transport in conjugated polymers occurs by thermally assisted hopping mechanism. Rate of this hopping process is governed by the reorganization energy consumed in geometrical rearrangement of molecules during a hopping event. Mobility of a DA copolymer can be varied over a large range by changing the length, composition, and position of the side chain.[7,8] This has been attributed to improved surface morphology, better alignment of polymer chains, as well as lower π–π stacking distance which enables a faster rate of inter-chain charge hopping.[9,10] The effect of presence of substituent groups and side chains on total reorganization energy, and consequent effect on mobility, has been studied previously.[11–13] However, the contribution of side chain

K. Patrikar, Prof. V. R. Rao
Department of Electrical Engineering
Indian Institute of Technology Bombay
Powai, Mumbai 400076, India
N. Jain, Prof. D. Kabra
Department of Physics
Indian Institute of Technology Bombay
Powai, Mumbai 400076, India
E-mail: dkabra@iitb.ac.in
D. Chakraborty, Prof. P. Johari
Department of Physics
School of Natural Sciences
Shiv Nadar University
Uttar Pradesh 201314, India
E-mail: priya.johari@snu.edu.in
The ORCID identification number(s) for the author(s) of this article can be found under https://doi.org/10.1002/adfm.201805878.

DOI: 10.1002/adfm.201805878

groups to the internal reorganization energy, and hence rate of charge transport, has not been explored much.

We have studied benzodithiophene (BDT)-thienothiophene (TT)-based DA copolymers PTB7 and PTB7-Th (also known as PBDTTT-EFT or PCE-10), with similar backbone molecular structure, however, composition differing only in the side chain pendant group.[14,15] Hence, these polymer systems are ideal for determining the role of pendant group on charge transport properties. Moreover, it has been found that OPV based on PTB7-Th has higher efficiency than PTB7 which has been attributed to lower reorganization energy of PTB7-Th-blended thin films.[16,17] While the fundamental differences in optical and photovoltaic device behavior of these polymers have been studied,[18] the differences in charge transport in the thin films of these polymers have not fully been explored. Takagi et al. have fabricated bottom-gate bottom-contact OFETs of PTB7 thin films and reported a field effect mobility of 2×10^{-3} cm^2 V^{-1} s^{-1}.[19] There are, however, no reports of PTB7-Th OFETs yet, to the best of our knowledge. We find a large difference in the field effect mobility of PTB7 and PTB7-Th. To understand the origin of this difference, reorganization energies are calculated for both of these systems to compare the behavior of these two materials at molecular level. The computed values are used to find the difference in rate of inter-chain charge transfer. We verify the trend in reorganization energy from external quantum efficiency (EQE) measurements of thin film of both polymers in the form of blends with $PC_{71}BM$, which is the common configuration of bulk heterojunction (BHJ) solar cells. Based on the theoretical calculations of reorganization energy and the measured values of field effect mobility, we calculate an effective charge hopping rate and charge transfer integral for PTB7 and PTB7-Th thin films.

2. Results

2.1. Devices of PTB7 and PTB7-Th

Molecular structures of PTB7 and PTB7-Th are shown in **Figure 1**a,b, respectively. The conjugated backbones for both polymers are identical. However, the pendant group has oxygen atom in PTB7, while it has thiophene unit in PTB7-Th. The UV–Visible absorption spectra of thin films of both polymers are shown in Figure S2 in the Supporting Information.

OFETs with PTB7 and PTB7-Th as channel were fabricated according to bottom-gate top-contact configuration with SiO_2–Poly (methyl methacrylate) (PMMA) bilayer dielectric, and MoO_3-Ag as source and drain electrodes, as per the thin film transistor schematic shown in Figure 1c. A typical example of the transfer (I_D–V_G) characteristics of PTB7 and PTB7-Th OFETs is shown in **Figure 2**a. It can be seen that the on-current of PTB7-Th OFET, 7.53 µA, is almost an order of magnitude higher than that of PTB7, 0.96 µA. Figure 2b shows the output (I_D–V_D) characteristics of a typical PTB7 and PTB7-Th thin film transistor. The devices exhibit I_D–V_D characteristics typical of OFETs, with linear current for low V_D and saturation at high V_D. Parameters extracted from transistors are shown in **Table 1**. Field-effect mobility in the saturated regime μ_{FET} was extracted from I_D–V_G characteristics shown in Figure S1a,b in the Supporting Information using Equation (1)[20]:

$$\mu_{FET} = \frac{1}{C_i}\left(\frac{\partial\sqrt{I_D}}{\partial V_G}\right)^2 \frac{2L}{W} \quad (1)$$

Here, C_i is the capacitance of dielectric stack (2 nF cm^{-2}, determined from C–V measurements). Length of channel (L)

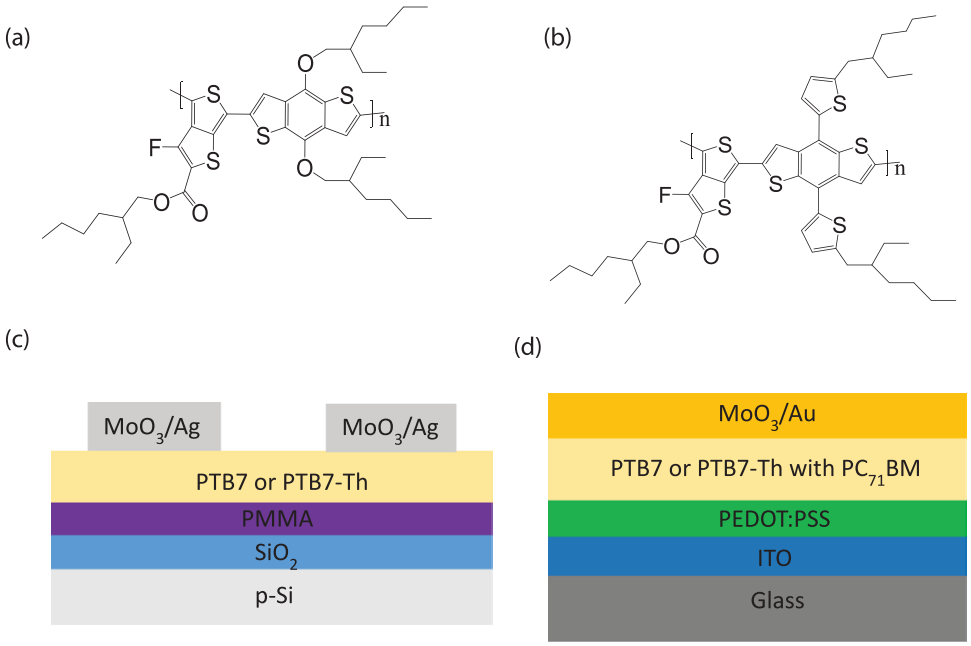

Figure 1. Schematic of molecular structure of a) PTB7 and b) PTB7-Th molecule. Device structure of fabricated c) field effect transistors and d) bulk heterojunction devices.

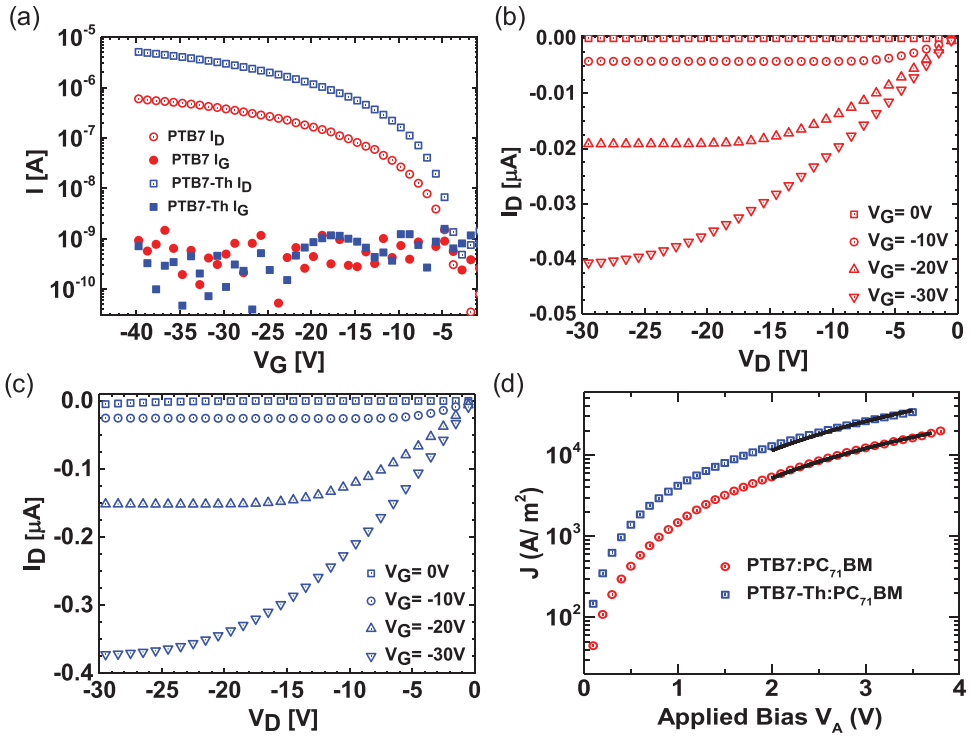

Figure 2. a) Transfer characteristics along with leakage current of PTB7 and PTB7-Th bottom-gate top-contact OFETs with SiO_2–PMMA bilayer dielectric and MoO_3-Ag source–drain electrodes. Output characteristics of typical b) PTB7 and c) PTB7-Th OFETs at V_G = 0, −10, −20, and −30 V. d) Current density versus applied voltage characteristics of BHJ devices with structure ITO/PEDOT:PSS/PTB7 or PTB7-Th and $PC_{71}BM/MoO_3$/Au.

is 75 μm, and width of channel (W) is 5 mm. μ_{FET} of PTB7 was found to be 0.01 ± 0.002 $cm^2\ V^{-1}\ s^{-1}$, which is an order of magnitude higher than the value previously reported for bottom-contact top-gate transistors with CYTOP as dielectric.[19] μ_{FET} for PTB7-Th thin film was found to be 0.11 ± 0.03 $cm^2\ V^{-1}\ s^{-1}$, an order of magnitude higher than that for PTB7. Threshold voltage determined from I_D–V_G characteristics, as shown in Figure S1c in the Supporting Information, are found to be close for both polymers, −11.05 V for PTB7 and −13.29 V for PTB7-Th. Methods for extraction of relevant device parameters from I_D–V_G characteristics of OFETs are discussed in Section S1 in the Supporting Information.

BHJ hole transport devices of PTB7 and PTB7-Th, in blends with $PC_{71}BM$, were fabricated according to the schematic shown in Figure 1d. Figure 2d shows the current density versus applied voltage (J–V_A) characteristics of PTB7 and PTB7-Th BHJ devices. J-V_A of BHJ devices represent the charge transport in direction perpendicular to the substrate. Space-charge limited current mobility (μ_{SCLC}) was extracted from J–V_A plots for BHJ devices of both the polymers using Equation (2)[21]:

$$J = \frac{9}{8}\mu_{SCLC}\varepsilon_0\varepsilon_r\frac{(V_A - V_{bi})^2}{d^3}\exp\left(\frac{\beta}{\sqrt{d}}\sqrt{V_A - V_{bi}}\right) \quad (2)$$

Here, J is the current density at applied bias of voltage V_A, ε_0 is the relative permittivity of space, ε_r is the dielectric constant of semiconductor, d is the thickness of semiconductor film, V_{bi} is the built-in potential, and β is the field-dependent parameter. The values calculated from these measurements are given in Table 1. J–V_A of BHJ devices represents the charge transport in direction perpendicular to the substrate. The values of μ_{SCLC} measured for PTB7 is 2.0×10^{-4} $cm^2\ V^{-1}\ s^{-1}$ and for PTB7-Th is 4.3×10^{-4} $cm^2\ V^{-1}\ s^{-1}$. The trend of higher mobility for PTB7-Th devices is seen in BHJ devices as well.

Table 1. Device parameters for PTB7 and PTB7-Th OFET and BHJ devices.

Material	OFET characteristics		BHJ characteristics
	Highest field effect mobility μ_{FET} [$cm^2\ V^{-1}\ s^{-1}$]	Threshold voltage V_{Th} [V]	SCLC mobility μ_{SCLC} [$cm^2\ V^{-1}\ s^{-1}$]
PTB7	0.012	−11.05	2.0×10^{-4}
PTB7-Th	0.143	−13.29	4.3×10^{-4}

2.2. Reorganization Energy of PTB7 and PTB7-Th

To gain further insight into the impact of molecular structure, viz. side chains on the charge transfer properties of these materials, the reorganization energy was calculated from the first-principles for both the polymers. Geometry of PTB7 and PTB7-Th molecules was optimized first. Key dihedral angles influencing the total energy of the systems are shown in **Figure 3**a,b. The angle between BDT, the pendant group, and ethylhexyl side chains ($\theta_{\perp 1}$) on one side and ($\theta_{\perp 2}$) on the other side were first manually fixed to various values starting

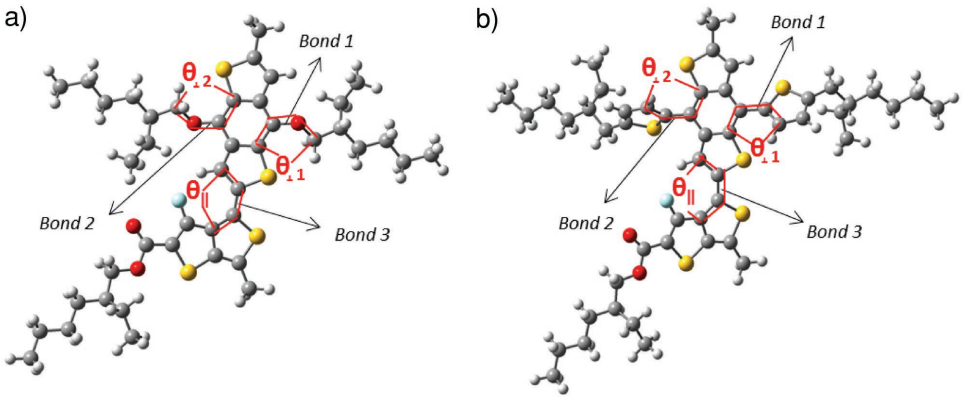

Figure 3. Key dihedral angles and bonds in a) PTB7 and b) PTB7-Th molecule used in computation. Values of these angles and bond lengths in neutral and cationic geometry are compared in Table 3.

from 10° to 60° with an interval of 10°. At this stage, the angle between BDT and TTT units ($\theta_{\|}$) was not allowed to relax. The optimized value of the perpendicular dihedral angles was found to be nearly 50° for both the molecules, as shown in Figure S3e,f in the Supporting Information with non-relaxed label. In the next step, $\theta_{\|}$ was allowed to relax for each of the earlier mentioned values of $\theta_{\perp 1}$ and $\theta_{\perp 2}$, results of which are shown in Figure S3e,f in the Supporting Information with relaxed label. Detailed results of geometry optimization are given in Tables S1 and S2 in the Supporting Information. Reorganization energy was calculated as the sum of two terms, referred to as λ_{1h} and λ_{2h}, computed values of which are given in Table S3 in the Supporting Information. λ_{1h} is the difference in energy between the relaxed configuration and rearranged configuration of ground state, and λ_{2h} is the difference in energy between the relaxed configuration and rearranged configuration of charged excited state[22] as shown in Figure S4 in the Supporting Information. The combination of λ_{1h} and λ_{2h} gives the hole reorganization energy, λ_h. The reorganization energy of PTB7-Th (150 meV) was found to be significantly lower than that for PTB7 (346 meV), as given in **Table 2**.

To understand the reason for a lower λ_h of PTB7-Th than PTB7, structural changes in respective molecules caused by addition of a hole, i.e., removal of an electron, to the neutral molecule were computed for both polymers. Differences in the bond lengths and bond angles, marked in Figure 3, between neutral and cationic molecule are summarized in **Table 3**. It can be seen that the differences in most geometric parameters between neutral and cationic structures are significantly lower for PTB7-Th than in PTB7. The bond length between pendant group and BDT (*Bond1*) extends by 0.031 Å in PTB7, more than twice the 0.012 Å extension in PTB7-Th. *Bond1* also undergoes more rotation in PTB7 than in PTB7-Th, as can be seen from difference in $\theta_{\perp 1}$ values, which are 19.6° and 4.63°, respectively. This shows that the presence of the thiophene unit in place of oxygen atom as pendant group makes PTB7-Th more rigid than PTB7. PTB7-Th thus undergoes less geometrical reorganization upon removal of a π-electron, requiring a lower reorganization energy.

We also extracted the reorganization energy from BHJ devices of PTB7 and PTB7-Th blends with $PC_{71}BM$ shown in Figure 1d.[23] The EQE versus energy of BHJ devices is shown in **Figure 4**. In the low energy range, the EQE at a given incident photon energy is governed by the conversion of charge transfer complex at the interface of polymer and $PC_{71}BM$. As this transfer causes physical rearrangement of the polymer, reorganization energy acts as an activation barrier in the process, analogous to the case of charge transfer between polymer chains. The relation of EQE and reorganization energy is given in Equation (3) as follows:

$$\mathrm{EQE}(E) \propto \frac{1}{E\sqrt{4\pi\lambda k_B T}} \exp\left(\frac{-(E_{CT}+\lambda-E)^2}{4\lambda k_B T}\right) \quad (3)$$

Here, λ is the reorganization energy for the polymer in the polymer–fullerene blend, k_B is the Boltzmann constant, and T is the temperature. E_{CT} is the energy of the interfacial charge transfer state, i.e., the diagonal band gap. The low energy region of EQE characteristics of blends with $PC_{71}BM$ of both polymers was fit according to Equation (3) to obtain reorganization energy. The values 0.2 eV for PTB7-Th and 0.31 eV for PTB7 blends follow the same trend as calculated values for molecules. This also reflects the observations of higher efficiency of PTB7-Th:$PC_{71}BM$ OPV; however, the focus of this paper is on charge transport properties of pure polymer films.

Table 2. Calculated values of reorganization energy and charge transfer parameters.

Material	Reorganization energy (DFT) λ_h [meV]	Reorganization energy (BHJ) λ [meV]	Normalized charge hopping rate kA^{-2} [s^{-1} eV^{-2}]	Effective inter-chain charge transfer rate k_{eff} [s^{-1}]	Effective charge transfer integral A_{eff} [meV]
PTB7	346.4	310.0	9.985×10^{14}	1.67×10^{11}	12.72
PTB7-Th	150.6	200.0	1.006×10^{16}	1.85×10^{12}	13.54

Table 3. Change in key geometric parameters (dihedral angles and bond lengths shown in Figure 3) on transition from neutral to cation geometry in PTB7 and PTB7-Th molecules.

	PTB7			PTB7-Th		
	Neutral	Cation	Change in bond length/Bond angle	Neutral	Cation	Change in bond length/Bond angle
$\theta_{\perp 1}$	47.99°	28.39°	19.6°	49.98°	45.35°	4.63°
$\theta_{\perp 2}$	48.81°	24.44°	24.37°	49.83°	42.98°	6.85°
$\theta_{\parallel}$	25.14°	19.35°	5.79°	26.55°	25.27°	1.28°
Bond 1	1.373 Å	1.342 Å	0.031 Å	1.467 Å	1.455 Å	0.012 Å
Bond 2	1.373 Å	1.342 Å	0.031 Å	1.467 Å	1.455 Å	0.012 Å
Bond 3	1.438 Å	1.427 Å	0.011 Å	1.441 Å	1.429 Å	0.012 Å

3. Discussions

As charge transport in organic materials occurs by a thermally assisted inter-chain hopping process,[32] mobility of charge carriers across a thin film depends directly on the rate of charge hopping between consecutive dimers. We have observed a consistent difference in FET mobility of PTB7 as an order of magnitude lower than PTB7-Th, which is an indication of a difference in rate of charge hopping in the respective polymer chains. To understand how a subtle difference in pendant group of polymer back bone has led to an order of magnitude difference in mobility, we seek to understand the phenomenon taking place in the polymer chains at molecular level during charge transfer. The kinetics and energetics of inter-chain charge transfer are quantified by Marcus theory.[24] Hole transfer is understood as a self-exchange reaction between identical dimers M_1 and M_2, as given in Equation (4)[25]:

$$M_1^+ + M_2 \rightarrow M_1 + M_2^+ \tag{4}$$

Rate of inter-chain hole transfer can be found by calculating rate of the reaction in Equation (4). As the dimers participating in hole transfer are identical, the activation barrier is solely governed by the reorganization energy for hole transfer (λ_h). The rate of this reaction can be expressed as an Arrhenius dependence on temperature (T), given in Equation (5)[22]:

$$k = \frac{A^2}{\hbar}\sqrt{\frac{\pi}{\lambda_h k_B T}}\exp\left(\frac{-\lambda_h}{4k_B T}\right) \tag{5}$$

Here, k is the rate of hole transfer and A is the charge transfer integral. k_B is the Boltzmann constant. Due to the Arrhenius nature of dependence on reorganization energy, a lower value of λ_h would mean a marked increase in the charge hopping rate of the material.

Charge transfer integral A represents the coupling between orbitals participating in the charge transfer reaction. Unlike λ_h, A is sensitive to area of orbital overlap of the HOMO of molecules participating in the charge transfer, and inter-chain distance in the thin film.[22] However, structure and composition of conjugated backbones of both polymers are identical. It can be seen in Figure S3c,d in the Supporting Information, that the HOMO orbitals participating in charge transport too are similar for both the molecules. The charge is mainly concentrated over the molecular backbone, especially donor BDT units, while pendant groups are involved as well. Difference in orbital area for both molecules is negligible. Further, X-ray-based studies have shown that the d-spacing in (010) direction, i.e., in the direction of charge transport, is similar for both polymers with 4.0 Å for PTB7 and 4.1 Å for PTB7-Th.[26,27] Due to these factors, it can be deduced that in Equation (5), A for both materials is equivalent.

Based on Equation (5), normalized rate of charge transfer kA^{-2} was calculated for both polymers using the λ_h values calculated from first-principles. We found that the values for PTB7 and PTB7-Th are $k_{PTB7}A^{-2} = 9.985 \times 10^{14}$ s^{-1} eV^{-2} and $k_{PTB7-Th}A^{-2} = 1.006 \times 10^{16}$ s^{-1} eV^{-2}, respectively. Thus, a difference of ≈200 meV in reorganization energy leads to the difference in normalized rate of transport by an order of magnitude. As A is equivalent for PTB7 and PTB7-Th (Table 2), this order of magnitude difference is essentially between k_{PTB7} and $k_{PTB7-Th}$. This corresponds to the order of magnitude difference observed in μ_{FET} for both polymers. Thus, we elucidate that λ_h is the key parameter that has led to the large difference in μ_{FET}. The ratio of BHJ μ_{SCLC} values for both polymers corresponds with λ estimated from EQE versus energy of the BHJ devices. This further affirms the role of reorganization energy in affecting mobility of these polymers.

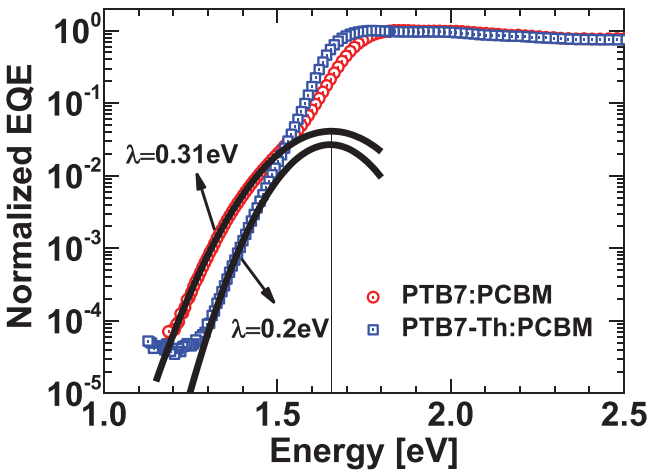

Figure 4. Normalized EQE characteristics of PTB7 and PTB7-Th thin films blended with $PC_{71}BM$ in device structure ITO/ZnO/PEIE/Blend/MoO_3/Ag. Reorganization energy (λ) extracted using Equation (3) for respective blends is in close agreement to trends found in estimation by first-principle calculation for PTB7 and PTB7-Th molecules.

Effective rate of hopping (k_{eff}) and effective charge transfer integral (A_{eff}) for the thin films were calculated using μ_{FET} obtained from devices and λ_h obtained from first-principles, according to Marcus theory. The detailed methods for the same are discussed in Section S2 in the Supporting Information. The values for k_{eff} and A_{eff} are given in Table 2. Difference in A_{eff} of both polymers was found to be less than 1 meV. Parameters k_{eff} and A_{eff} are obtained from the measured value of mobility which is a thin-film property, and the calculated value of reorganization energy which is a molecular property. Hence, they correlate the local inter-chain charge hopping to the charge transport observed within the OFET channel.

4. Conclusion

We studied the charge transport properties of DA polymers PTB7 and PTB7-Th. The field-effect mobility of PTB7-Th was observed to be ≈10 times higher than that of PTB7. We attribute the vast difference in field-effect mobility in PTB7 and PTB7-Th polymer thin films to the difference in reorganization energy of the two molecules. We found a significant difference in the reorganization energy values calculated from first-principles for both the molecules, and showed that the ratio of rate of inter-chain charge hopping obtained from these is ≈10. We found that replacing oxygen with thiophene unit in the pendant group imparts rigidity to the polymer that leads to the large difference in reorganization energy. Using measured values of FET mobility and first-principles values of reorganization energy, we calculated an effective charge transfer integral for PTB7 and PTB7-Th thin films, which had similar values for both polymers. PTB7 and PTB7-Th have identical molecular structure except the pendant groups. However, this leads to a significant difference in reorganization energy, and consequently field-effect mobility of thin films. This opens a new paradigm regarding the role of side group/chain in influencing the charge transport properties of conjugated polymers.

5. Experimental Section

Device Fabrication: Transistors for field-effect mobility measurements were fabricated on low-resistivity p-type (100) silicon substrates, which also acted as the gate electrode. A 180 nm thermal oxide was grown on surface to form the dielectric. PMMA was deposited on the oxide by spin coating from a 2% solution in anisole at 2000 rpm for 60 s, followed by a 20 min annealing at 200 °C. Thickness of the PMMA layer was approximately 100 nm as determined by ellipsometer measurement. Details of the PMMA deposition are given in Section S3 in the Supporting Information. Substrates were then transferred to a nitrogen environment in an MBraun glove box. Polymers PTB7 and PTB7-Th were spin coated on this composite dielectric from chlorobenzene solutions (10 mg mL^{-1}) heated to 70 °C, at 2000 rpm for 60 s. 1,8-Diiodooctane (10 µL) had been added to the solutions. Spin coating was followed by annealing for 10 min at 70 °C. Stack of 5 nm MoO_3 capped by 40 nm Ag layer acted as source–drain contacts. These electrodes were deposited by thermal evaporation, through stencil masks with minimum channel length of 75 µm. BHJ devices were fabricated on indium tin oxide (ITO) coated glass substrates. PEDOT:PSS was spin coated on ITO before transferring substrates to nitrogen environment in an MBraun glove box. Polymers PTB7 and PTB7-Th blended with $PC_{71}BM$ in ratio 1:1.5 by weight in chlorobenzene solutions (25 mg mL^{-1}) were spin coated at 2000 rpm for 60 s. This was followed by thermal evaporation of 5–40 nm MoO_3-Au bilayer for top electrodes through shadow masks of length 3 mm and width 1.5 mm.

Electrical Measurements: Electrical measurements on all devices were done in nitrogen environment in an MBraun glove box at room temperature, using a semiprobe station unit with Keithly 4200 Semiconductor Characterization System.

Computational Methods: Geometry optimizations and reorganization energy calculations were done using plane wave basis sets in VASP[28] with PAW-PBE exchange-correlation functional.[29–31] A vacuum of 12 Å in all three directions was introduced to realize the molecular structure within the framework of periodic boundary conditions, so that one molecular unit could not interact with its mirror image in any of the three directions. The convergence for energy in all calculations was set to 10^{-4} eV between two steps and the structures were relaxed until the maximum Hellmann–Feynman forces acting on each atom reached the value of ≤0.01 eV Å^{-1} upon the ionic relaxation. An energy cutoff of 520 eV for plane wave basis set was used for all the calculations. All the calculations were performed using a single *k*-point in Brillouin zone (BZ), i.e., at the Γ-point.

Supporting Information

Supporting Information is available from the Wiley Online Library or from the author.

Acknowledgements

The authors acknowledge (DST–AISRF) for partial funding for this project. The authors also acknowledge the support from NCPRE IIT Bombay for device fabrication and characterizations facility. D.C. and P.J. would like to acknowledge the high-performance computing facility and workstations available at the School of Natural Sciences, Shiv Nadar University, which were used to perform all calculations. N.J. acknowledges the Council of Scientific and Industrial Research (CSIR), India, for fellowship. KP acknowledges Centre for Excellence in Nanoelectronics IIT Bombay for fellowship.

Conflict of Interest

The authors declare no conflict of interest.

Keywords

mobility, OFET, pendant groups, reorganization energy

Received: August 22, 2018
Revised: November 23, 2018
Published online:

[1] A. Nigam, D. Kabra, T. Garg, M. Premaratne, V. R. Rao, *Org. Electron. Phys., Mater. Appl.* **2015**, *22*, 202.
[2] N. Chandrasekaran, E. Gann, N. Jain, A. Kumar, S. Gopinathan, A. Sadhanala, R. H. Friend, A. Kumar, C. R. McNeill, D. Kabra, *ACS Appl. Mater. Interfaces* **2016**, *8*, 20243.
[3] S. Zhang, Y. Qin, J. Zhu, J. Hou, *Adv. Mater.* **2018**, *30*, 1.
[4] Z. G. Zhang, J. Wang, *J. Mater. Chem.* **2012**, *22*, 4178.
[5] Q. Wan, X. Guo, Z. Wang, W. Li, B. Guo, W. Ma, M. Zhang, Y. Li, *Adv. Funct. Mater.* **2016**, *26*, 6635.
[6] L. Biniek, B. C. Schroeder, C. B. Nielsen, I. McCulloch, *J. Mater. Chem.* **2012**, *22*, 14803.

[7] S. Chen, B. Sun, W. Hong, H. Aziz, Y. Meng, Y. Li, *J. Mater. Chem. C* **2014**, *2*, 2183.
[8] I. Kang, H. Yun, D. S. Chung, S. Kwon, Y. Kim, *J. Am. Chem. Soc.* **2013**, *135*, 14896.
[9] Y. Olivier, D. Niedzialek, V. Lemaur, W. Pisula, K. Müllen, U. Koldemir, J. R. Reynolds, R. Lazzaroni, J. Cornil, D. Beljonne, *Adv. Mater.* **2014**, *26*, 2119.
[10] J. Mei, Z. Bao, *Chem. Mater.* **2014**, *26*, 604.
[11] H. Geng, Y. Niu, Q. Peng, Z. Shuai, V. Coropceanu, J. L. Brédas, *J. Chem. Phys.*104703, **2011**, *135*.
[12] G. R. Hutchison, M. A. Ratner, T. J. Marks, *J. Am. Chem. Soc.* **2005**, *127*, 2339.
[13] M. Gruber, S. H. Jung, S. Schott, D. Venkateshvaran, A. J. Kronemeijer, J. W. Andreasen, C. R. McNeill, W. W. H. Wong, M. Shahid, M. Heeney, J. K. Lee, H. Sirringhaus, *Chem. Sci.* **2015**, *6*, 6949.
[14] Y. Liang, Z. Xu, J. Xia, S. T. Tsai, Y. Wu, G. Li, C. Ray, L. Yu, *Adv. Mater.* **2010**, *22*, E135.
[15] S. H. Liao, H. J. Jhuo, Y. S. Cheng, S. A. Chen, *Adv. Mater.* **2013**, *25*, 4766.
[16] N. Jain, N. Chandrasekaran, A. Sadhanala, R. H. Friend, C. R. McNeill, D. Kabra, *J. Mater. Chem. A* **2017**, *5*, 24749.
[17] K. D. Deshmukh, S. K. K. Prasad, N. Chandrasekaran, A. C. Y. Liu, E. Gann, L. Thomsen, D. Kabra, J. M. Hodgkiss, C. R. McNeill, *Chem. Mater.* **2017**, *29*, 804.
[18] F. Bencheikh, D. Duché, C. M. Ruiz, J. J. Simon, L. Escoubas, *J. Phys. Chem. C* **2015**, *119*, 24643.
[19] K. Takagi, T. Nagase, T. Kobayashi, H. Naito, *Jpn. J. Appl. Phys.* **2014**, *53*, 050305.
[20] G. Horowitz, P. Delannoy, *J. Appl. Phys.* **1991**, *70*, 469.
[21] P. N. Murgatroyd, *J. Phys. D: Appl. Phys.* **1970**, *3*, 151.
[22] P. F. Barbara, T. J. Meyer, M. A. Ratner, *J. Phys. Chem.* **1996**, *100*, 13148.
[23] K. Vandewal, K. Tvingstedt, A. Gadisa, O. Inganäs, J. V. Manca, *Phys. Rev. B* **2010**, *81*, 1.
[24] R. A. Marcus, *Angew. Chem., Int. Ed.* **1993**, *32*, 1111.
[25] Y. A. Berlin, G. R. Hutchison, P. Rempala, M. A. Ratner, J. Michl, *J. Phys. Chem. A* **2003**, *107*, 3970.
[26] W. Huang, E. Gann, L. Thomsen, C. Dong, Y. B. Cheng, C. R. McNeill, *Adv. Energy Mater.* **2015**, *5*, 1.
[27] B. A. Collins, Z. Li, J. R. Tumbleston, E. Gann, C. R. Mcneill, H. Ade, *Adv. Energy Mater.* **2013**, *3*, 65.
[28] G. Kresse, J. Furthmüller, *Phys. Rev. B* **1996**, *54*, 11169.
[29] D. Joubert, *Phys. Rev. B* **1999**, *59*, 1758.
[30] D. Vanderbilt, *Phys. Rev. B* **1990**, *41*, 7892.
[31] J. P. Perdew, K. Burke, M. Ernzerhof, *Phys. Rev. Lett.* **1996**, *77*, 3865.
[32] H. Bässler, A. Köhler, in *Unimolecular and Supramolecular Electronics I. Topics in Current Chemistry*, Vol. *312* (Eds: R. Metzger), Springer, Berlin, Heidelberg **2011**.